

Tribology Analysis of Chemical-Mechanical Polishing

To cite this article: Scott R. Runnels and L. Michael Eyman 1994 *J. Electrochem. Soc.* **141** 1698

View the [article online](#) for updates and enhancements.

You may also like

- [Passive Film Structure of Supersaturated AlMo Alloys](#)
G. D. Davis, W. C. Moshier, G. G. Long et al.
- [Characterization of the Chemical Mechanical Polishing Process Based on Nanoindentation Measurement of Dielectric Films](#)
ChiWen Liu, BauTong Dai and ChingFa Yeh
- [Radiotracer Studies of Metal Ion Exchange Inhibition Using Organic Inhibitors](#)
Sally Shinew Twining and David S. Newman



Your Lab in a Box!

The PAT-Tester-i-16: All you need for Battery Material Testing.

- ✓ All-in-One Solution with integrated Temperature Chamber!
- ✓ Cableless Connection for Battery Test Cells!
- ✓ Fully featured Multichannel Potentiostat / Galvanostat / EIS!

www.el-cell.com +49 40 79012-734 sales@el-cell.com


electrochemical test equipment



17. G. Stoney, *Proc. R. Soc. London Ser. A*, **82**, 172 (1909).
18. W. A. Brantley, *J. Appl. Phys.*, **44**, 534 (1973).
19. B. Jönsson and S. Hogmark, *Thin Solid Films*, **114**, 257 (1984).
20. J. J. Cuomo and R. J. Gambino, *J. Vac. Sci. Technol.*, **14**, 152 (1977).
21. G. Carter and D. G. Armour, *Thin Solid Films*, **80**, 13 (1981).
22. K. J. Close and J. Yarwood, *Brit. J. Appl. Phys.*, **18**, 1593 (1967).
23. A. Gittis and D. Dobrev, *Thin Solid Films*, **130**, 335 (1985).
24. F. M. d'Heurle and J. M. E. Harper, *ibid.*, **171**, 81 (1989).
25. K. Fuchs, *Proc. Cambridge Philos. Soc.*, **34**, 100 (1938).
26. E. H. Sondheimer, *Adv. Phys.*, **1**, 1 (1952).
27. N. M. Ashcroft and N. D. Mermin, *Solid State Physics*, HRW International Editions, Saunders, Philadelphia (1976).
28. A. F. Mayadas and M. Shatzkes, *Phys. Rev. B*, **1**, 1382 (1970).
29. J. M. Ziman, in *The Physics of Metal*, J. M. Ziman, Editor, p. 264, Cambridge University Press, Cambridge (1969).
30. W. A. Harrison, *Electronic Structure and the Properties of Solids*, Freeman, San Francisco (1980).

Tribology Analysis of Chemical-Mechanical Polishing

Scott R. Runnels* and L. Michael Eyman

Sematech, Austin, Texas 78741-6499

ABSTRACT

To better understand the variation of material removal rate on a wafer during chemical-mechanical polishing (CMP), knowledge of the stress distribution on the wafer surface is required. The difference in wafer-surface stress distributions could be considerable depending on whether or not the wafer hydroplanes during polishing. This study analyzes the fluid film between the wafer and pad and demonstrates that hydroplaning is possible for standard CMP processes. The importance of wafer curvature, slurry viscosity, and rotation speed on the thickness of the fluid film is also demonstrated.

Chemical-mechanical polishing (CMP) is receiving increased attention as a method for silicon wafer planarization that can meet the more stringent lithographic requirements of planarity for future submicron device manufacturing. In the CMP process, a wafer is rotated about its axis while being pressed face-down by a "carrier" against a rotating polish pad covered with colloidal silica slurry. The relative motion of the wafer and pad combined with the applied pressure and chemical activity of the slurry erodes features on the wafer.

Achieving highly uniform material removal is a primary goal of CMP and has proven to be difficult. There are several process variables that affect uniformity, such as polish pad and wafer carrier rotational velocities, pad conditioning, and the type of slurry. Statistical methods can be used to design experiments to distinguish the effects of these variables on material removal rate and uniformity, but none have been successfully used to characterize the process in a robust way. Hence, although the effects of changes in process variables can be quantified, there is little understanding of the nature of their effects. This lack of understanding will ultimately limit the ability of experimentally based statistical methods to improve the process, therefore statistical studies must eventually be augmented with a deeper understanding of polishing physics and chemistry.

Because there is a variety of physical mechanisms that are involved in CMP, there is a need for analyses from various science and engineering fields. From the field of glass science, which has significant overlap with CMP of silicon oxides, Cook¹ provides a good summary of microscopic-scale analytical models of polishing that lend insight into possible erosion mechanisms. From the field of continuum mechanics, elasticity modeling of polish pad deformation² has indicated that removal nonuniformities within 1 mm of the wafer edge may be attributable to pad stresses. Nakamura³ demonstrated the use of standard tribology models to develop a "bowl-feed" process for CMP. Other more empirical modeling approaches are those of Warnock⁴ and Preston.⁵

Background

CMP enhances the natural etching caused by the slurry through abrasion of the wafer surface. Thus, the basis of

this study is the hypothesis that a material removal model can be formed using the wafer surface stress distribution, which is responsible for the abrasion that forces material off the wafer. The most common model for material removal is Preston's equation⁵ where removal rate R is related to pressure P and relative velocity V between the pad and wafer as

$$R = kP||V|| \quad [1]$$

Although Preston's equation has been used with some success to model overall material removal, it fails to provide a robust model over a wide range of process parameters. This is because the wafer-surface stress distribution is only represented implicitly through the effects of applied pressure and relative velocity when, in reality, the relationship between them and the wafer surface stresses could change dramatically depending on the process parameters. In particular, the relative velocity's effect on wafer-surface shear stress when the wafer slides directly against the pad would be quite different than when the wafer hydroplanes on a thin film of slurry. For this reason, the present tribology analysis is performed to improve the understanding of the wafer-pad interface.

The field of tribology has delineated three scenarios that characterize any solid-solid interface involving a lubricating fluid and relative sliding motion.⁶ The first scenario is direct contact where the load between the two surfaces is supported almost entirely through solid structures. The second scenario is semidirect contact where there remains some solid contact, but the fluid between the surfaces also partially supports the load. The third scenario is hydrodynamic lubrication where the load is supported only by a fluid layer, and thus the nature of stress transferral is markedly different than that of solid contact.

A more complete removal rate model, based on our hypothesis, would be of the form $R = f(\sigma, \tau)$ where σ and τ are the magnitudes of the normal and shear stresses, respectively, on the wafer surface. An analogy to Preston's equation would be the model

$$R = \hat{k}\sigma\tau \quad [2]$$

The development and use of such models requires the determination of stress distributions, a task that involves representing several mechanisms including fluid flow and solid

* Electrochemical Society Active Member.

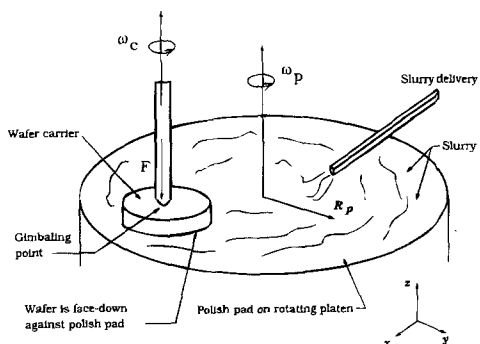


Fig. 1. Schematic of CMP process.

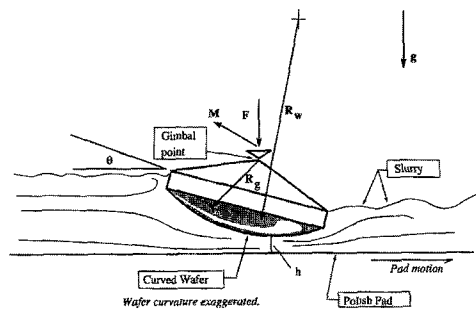


Fig. 2. Schematic representation of tribology modeling.

deformation. The focus of the present study is the contribution of the fluid mechanics to the stresses. Their contribution is investigated by simulating the flow of a thin layer between the wafer and pad. The existence of the layer is an initial assumption for the analysis and evaluating the validity of this assumption is the primary focus.

Modeling Procedures

Figure 1 is a schematic of the CMP configuration. Figure 2 illustrates the scope of the present investigation. A wafer of radius 10 cm and spherical curvature R_w rotates about its axis of symmetry, which is approximately 30 cm from the pad's rotational axis. The wafer glides at an angle of attack θ upon a slurry film whose minimum thickness is denoted by h . The wafer's angle of attack and curvature together with the motion of the pad form a converging flow of slurry under the wafer that enables the flow to support the load of the wafer in a way similar to that of a bearing. The wafer carrier is mounted on a gimbal mechanism which allows the carrier to adjust during polishing to prevent the wafer snagging on the pad. The vector \mathbf{R}_g identifies the position of any point on the wafer's surface measured from the gimbaling point.

The modeling procedure focuses on the flow in the gap. The flow simulation is embedded in an iterative scheme for determining the correct h and θ values that will cause the film to correctly support the carrier and applied load. The fluid flow simulation is discussed below after which the iterative scheme for determining h and θ is described.

Simplifications for flow modeling.—A fundamental assumption of the fluid film model is that the wafer and pad are rigid and smooth. Hence the pad is flat, and the wafer curvature radius R_w is constant for a given study. This means that additional frictional effects from pad roughness, which are known to result in significant variations in material removal rates and uniformity, are not incorporated directly. However, as described later, the effects of pad roughness are used in the evaluation of the tribology results. As will be described in the next section, the pad and wafer are simply represented as boundaries to the flow region on which no-slip velocity boundary conditions are imposed. A pad deformation analysis² lends support to modeling the pad as rigid, indicating that the pad deflects less than 3 μm under standard CMP loads. However, the as-

sumption that the wafer is rigid may be less valid, and so the effect of curvature on the fluid layer is also investigated. One other simplification for the flow modeling is that the colloidal silica slurry (which contains particles on the order of 1 μm) is represented as a Newtonian fluid with constant viscosity even though it is known to exhibit non-Newtonian behavior. In addition to these simplifications, there are others made in the iterative process for determining the film that will be discussed later.

Governing equations and boundary conditions.—The fluid flow in the pad-wafer interface is represented by the steady-state three-dimensional Navier-Stokes equations for incompressible Newtonian flow with constant viscosity given below

$$\mathbf{u} \cdot \nabla \mathbf{u} = -\frac{1}{\rho} \nabla p + \frac{\mu}{\rho} \nabla^2 \mathbf{u}$$

$$\nabla \cdot \mathbf{u} = 0$$

where ρ is the density, μ is the dynamic viscosity, p is the pressure, and \mathbf{u} is the vector-valued velocity at any point in the flow. The solution domain for the equations is shown with boundary conditions in Fig. 3. The domain consists of a very thin disk of fluid (representing the fluid in the pad-wafer interface) surrounded by a ring (representing flow around the outside of the carrier). On the bottom of the thin disk, no-slip velocity boundary conditions are applied that represent the velocity of the pad and is equal to $\mathbf{R}_p \times \omega_p$ (see Fig. 1). On the top of the thin disk and on the interior side walls, no-slip velocity boundary conditions are applied that represent the velocity of the wafer and carrier. The velocity field at any point on these surfaces is equal to $\mathbf{R}_g \times \omega_c$, where \mathbf{R}_g points from the gimbaling point to any point on the rotating wafer or carrier (see Fig. 1 and 2). On the remaining surfaces, zero-stress boundary conditions are applied that allow fluid to enter and leave the domain freely. In principle this ring could be extended to encompass all the slurry above the pad, but this is unnecessary and would greatly increase the computation time.

The governing equations together with the boundary conditions form a well-posed boundary value problem. The solution is approximated using the Galerkin finite element method. The aspect ratios in the wafer-pad interface (centimeters radially and microns vertically) require very flat elements and thus present a challenge for the finite element mesh generation and solutions steps. A three-dimensional mesh consisting of over 5000 linear elements was developed and used to obtain satisfactory solutions.

Procedure for determining the fluid layer.—There are two conditions that the fluid layer in the model must satisfy. First, it must support the wafer carrier and applied load during polishing. Figure 2 illustrates the resultant vector due to the carrier weight and the applied load. The force on the wafer surface from the fluid flow is given by

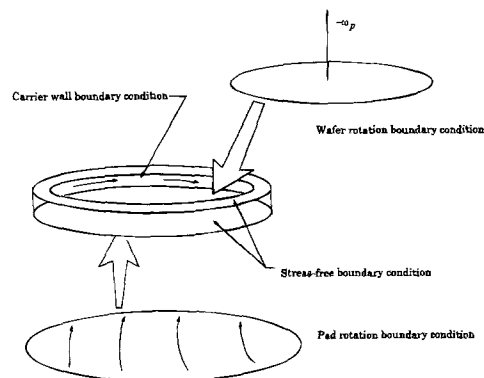


Fig. 3. Schematic representation of solution domain and boundary conditions.

$$\mathbf{F}_t = \int_{\text{wafer surface}} \boldsymbol{\sigma} \cdot \mathbf{n} dA \quad [3]$$

where the stress tensor $\boldsymbol{\sigma}$ is related to the flow field by

$$\sigma_{ij} = -p\delta_{ij} + \mu \left(\frac{\partial u_i}{\partial x_j} + \frac{\partial u_j}{\partial x_i} \right) \quad [4]$$

δ_{ij} is the Kronecker delta, and \mathbf{n} is the surface normal. F_t , the vertical component of \mathbf{F}_t , is required to equal that of \mathbf{F} in the iterative procedure described at the end of this section.

The second condition is that the fluid film be stable. This requires the moment of the force from the fluid film to have components which are zero in the plane perpendicular to the carrier's axis of rotation since the gimbal mechanism cannot support moments in these directions. To reduce the amount of iteration performed for determining the fluid layer, this requirement is relaxed in that only the component perpendicular to the page (*i.e.*, that associated with the angle of attack, θ) in Fig. 2 is required to be zero. This is the component that could cause the wafer carrier to snag on the pad and is thus considered to be the most important in terms of stability. The other component of the moment could also be considered, in principle, with another rotation angle on the corresponding axis introduced as a parameter to be varied. The moment about the gimbal point from the fluid flow is computed as

$$\mathbf{M}_t = \int_{\text{wafer surface}} \mathbf{R}_g \times \boldsymbol{\sigma} \cdot \mathbf{n} dA \quad [5]$$

M_t , the component of \mathbf{M}_t associated with θ , is required to be zero in the iterative process described below.

There are three parameters that describe the shape of the fluid film: the minimum thickness of the film (h), the wafer angle of attack (θ), and the wafer's radius of curvature (R_w). Since the wafer is assumed rigid, R_w is constant for a particular case. Then, given the two variable parameters h and θ , the procedure for determining the film is as follows: (i) assume a particular fluid layer exists which is defined by the wafer's radius of curvature R_w , minimum thickness h , and wafer angle of attack θ , (ii) compute the fluid flow in that layer during polishing, (iii) compute F_t and M_t , and (iv) if $|F_t - F| = |M_t| = 0$, then stop. If not, adjust the fluid layer by varying h and θ and go to step 2.

The fluid layer that emerges from the iterative procedure must be evaluated in the context of the assumptions made in determining it. Specifically, since the wafer and pad were both represented as smooth, the thickness of the resulting fluid layer must be appreciably larger than the average feature height on real wafers and pads. For example, if the above procedure predicts a relatively thick fluid film, the smoothness assumption is justified, but if it predicts a relatively thin one, the smoothness assumption is questionable. Therefore, the fluid thickness and the pad condition must be considered together when evaluating the predictions of the model.

Results

Base-line case.—A base-line case is considered first where the rotation speeds are 20 rpm, and the slurry viscosity is 0.0214 kg m/s. The "dome-height" is the distance the center of the wafer protrudes past its perimeter and is a more convenient measure of wafer curvature than its radius of curvature since the radius of curvature is quite large (500 m). For the base-line case, the dome height was 10 μm . The loading conditions for all the studies is 352 lb, which corresponds to an average pressure of 7 psi. The plots in Fig. 4 and 5 show how the vertical force and moment varies with θ for various h values. The loading data shown in Fig. 4 may be extrapolated/interpolated to define a set of (h , θ) pairs that satisfies the load condition of 352 lb. The same procedure may be applied to the moment data shown in Fig. 5 to define a set of (h , θ) pairs that satisfies the zero moment condition. The functions defined by these two sets of (h , θ) pairs are plotted in Fig. 6. Their intersection point indicates that $h \approx 63 \mu\text{m}$ and $\theta \approx 0.01$ degrees simultaneously satisfies the load and moment conditions. More-

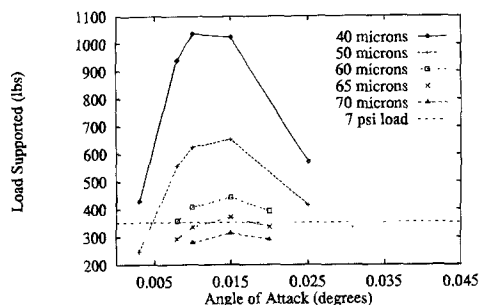


Fig. 4. Moment about gimbal due to fluid flow at pad-wafer interface for base-line case.

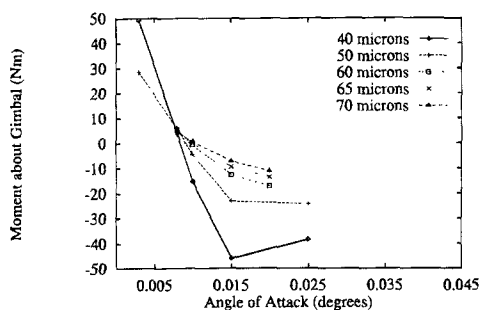


Fig. 5. Supported load due to fluid flow at pad-wafer interface for base-line case.

over, in Fig. 5 it is observed that this (h , θ) pair is stable in that a perturbation in θ causes a moment which is self-correcting. It is also noted that the minimum gap thickness of 65 μm is significantly larger than standard pad and wafer features indicating the likelihood of a fluid layer at the interface.

Parametric studies.—Because of the approximations in the model, it is difficult to extract quantitative values from the results. The most useful information that can be obtained from the model is the sensitivity of the film to cer-

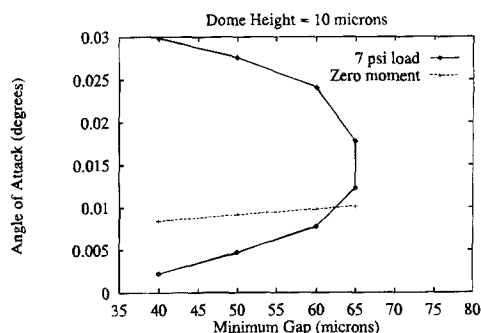


Fig. 6. Plot of (h , θ) pairs which satisfy either the loading or moment conditions for the base-line case.

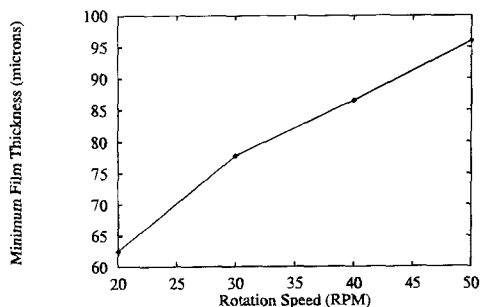


Fig. 7. Dependence of film thickness on speed.

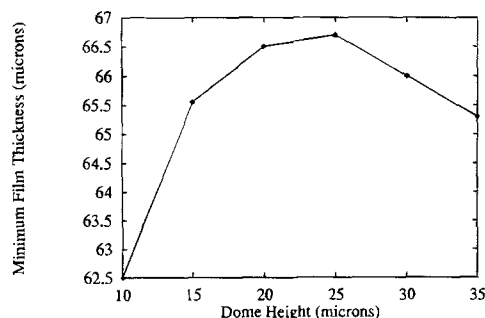


Fig. 8. Dependence of film thickness on wafer curvature.

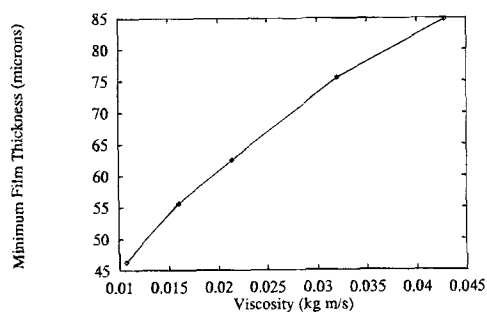


Fig. 9. Dependence of film thickness on viscosity.

tain process parameters such as wafer curvature, slurry viscosity, and rotation speed.

The above process for determining the stable (h , θ) pairs was repeated for various sets of process parameters. The results are presented in terms of minimum film thickness as a function of a varied parameter. The minimum film thickness is an important measure of the film since it, compared to the feature sizes on the pad and wafer, will determine if there is a film present. The following parametric studies will demonstrate that the process parameters of speed, viscosity, and wafer curvature each may be a determining factor for the existence of the fluid layer.

Figure 7 shows that the minimum film thickness exhibits a sublinear variation with respect to speed. The figure also indicates the importance of rotational speed in relation to the existence of a fluid film since it shows a 40% variation in film thickness over common CMP speeds.

Next, the effect of wafer curvature on the minimum film thickness is shown in Fig. 8. As the curvature of the wafer is increased, larger angles of attack are required to satisfy the zero-moment condition. And, since larger angles of attack require thicker films to match the load, increasing wafer curvature increases the film thickness. For large enough curvatures, however, the flow is not able to sustain high enough pressures to offset the increased protrusion of the wafer thus leading to a decrease in minimum film thickness. Although the magnitude of the variation in film thickness with dome height is small (less than 10%) for the range studied, the trend in film thickness at smaller dome heights indicates that changes in curvature from 5 to 10 μm may lead to dramatic changes in the film. This is an important result because methods for establishing and maintaining highly accurate and stable wafer curvature are not yet a standard part of CMP processes and may, in fact, be difficult to achieve. Also, wafer warp and bow have been meas-

ured to be approximately 10 μm in some cases,⁷ and could thus be additional factors affecting the film.

Finally, the effect of viscosity on the change in minimum film thickness is plotted in Fig. 9. The magnitude of the variation in this result is important when one considers that changes in viscosity due to ordinary temperature ranges experienced by the slurry during polishing may be as much as 30%. This result indicates that such a variation could cause a change in film thickness of around 20%. Of more importance, however, this result implies that the dependence of the film on viscosity is especially pertinent when evaluating new slurries. Specifically, as different slurries are developed to enhance their chemical properties, the variation in polishing characteristics which they produce must also be attributed to their effect on the film thickness.

Conclusion

The tribology analysis presented here demonstrates that the effects of some process parameters on the existence of the fluid layer at the pad-wafer interface are profound. Because of the approximations in the model, it is inappropriate to use the numerical results as quantitative predictions of the film thickness. Nevertheless, the trends indicated by the parametric studies are compelling. The effect of these parameters on the nature and possibly the very existence of the fluid layer may partly explain why the CMP process is so difficult to characterize. The trends indicate that the wafer-pad interface is a very delicate balance between hydrodynamic lubrication, mixed solid-liquid contact, and possibly even some direct solid-solid contact.

One may speculate that hydrodynamic lubrication is responsible for distributing the slurry, and solid-solid contact is responsible for the majority of the material removal, and then conclude that this balance is crucial to the process. However, even if this hypothesis is correct, maintaining such a delicate balance in the interface will continue to be a difficult challenge for CMP. Thus it may be wise to consider alternative designs that allow even and predictable distribution of slurry along with the required solid-solid abrasive contact. If the process could be modified to produce a more stable interface, then it could be more clearly characterized and thus controlled and optimized for better CMP performance.

Acknowledgments

The authors would like to thank Anthony Toprac for proofreading the manuscript, along with Mukesh Desai and Rahul Jairath for their comments.

Manuscript submitted Aug. 11, 1993; revised manuscript received Feb. 7, 1994.

SEMATECH, Incorporated, assisted in meeting the publication costs of this article.

REFERENCES

1. L. Cook, *J. Non-Crystalline Solids*, **120**, 152 (1990).
2. S. R. Rannels and P. Renteln, *Dielectric Sci. Technol.* (1993).
3. K. Akamatsu, T. Nakamura, and N. Arakawa, *Bull. Jpn. Soc. Prec. Engg.*, **19**, 120 (1985).
4. J. Warnock, *This Journal*, **138**, 2398 (1991).
5. F. Preston, *J. Soc. Glass Technol.*, **11** (1927).
6. G. M. Bartenev and V. V. Lavrentev, *Friction and Wear of Polymers*, Elsevier Scientific Publishing Co., New York (1981).
7. G. H. Popham, H. R. Huff, and R. W. Potter, *This Journal*, **140**, 229 (1993).